pharmaceutics

MDPI

Article

Mixture-Design Optimization of an Intranasal Self-Nanoemulsifying Drug Delivery System Co-Loaded with Olmesartan Medoxomil and Apigenin: Composition Modeling and Ex Vivo Nasal Permeation

Ehab M. Elzayat *, Sultan Almutairy, Abdelrahman Y. Sherif, Mohamed M. Badran and Mohammad A. Altamimi *

Kayyali Chair for Pharmaceutical Industries, Department of Pharmaceutics, College of Pharmacy, King Saud University, Riyadh 11451, Saudi Arabia; 446100129@student.ksu.edu.sa (S.A.); ashreef@ksu.edu.sa (A.Y.S.); mbadran@ksu.edu.sa (M.M.B.)

* Correspondence: eelzayat1.c@ksu.edu.sa (E.M.E.); maltamimi@ksu.edu.sa (M.A.A.)

Abstract

Background/Objectives: Ischemic brain injury involves parallel oxidative, inflammatory, and vascular cascades. Olmesartan medoxomil and apigenin act on complementary arms and can serve this purpose. This study developed a self-nanoemulsifying drug delivery system (SNEDDS) co-loaded with both agents for intranasal use. Constrained mixture design was used to determine its actual composition. **Methods:** Oil and cosolvent were selected by saturation solubility and surfactant by emulsification transmittance. The proportions of Kolliphor EL (40–70% *w*/*w*), poly(ethylene glycol) 400 (5–30% *w*/*w*), and Imwitor 308 (20–40% *w*/*w*) were treated as mixture variables and each drug's solubility as the response. Desirability analysis identified the optimum composition, which was experimentally verified. After that, it was compared with a drug suspension for permeation across excised goat nasal mucosa in Franz diffusion cells. **Results:** Apigenin solubility followed a linear mixture model and olmesartan medoxomil a quadratic model. The optimum composition (52.33% Kolliphor EL, 27.67% poly(ethylene glycol) 400, 20.00% Imwitor 308) gave observed solubilities of 11.82 and 6.91 mg/g, within the 95% prediction intervals. Steady-state flux rose from 0.85 ± 0.68 to 8.46 ± 2.51 μg/cm^2/h for olmesartan medoxomil and from 0.18 ± 0.17 to 10.06 ± 3.63 μg/cm^2/h for apigenin. **Conclusions:** A constrained mixture design identified a SNEDDS composition that accommodated both drugs and markedly increased their transport across excised nasal mucosa relative to a suspension. These findings establish a formulation basis for the intranasal administration of this drug combination.

Keywords: self-nanoemulsifying drug delivery system; constrained mixture design; olmesartan medoxomil; apigenin; intranasal delivery; ex vivo nasal permeation; Kolliphor EL; desirability optimization

Check for updates

Academic Editor: Diego Romano Perinelli

Received: 30 September 2026
Revised: 7 November 2026
Accepted: 14 November 2026
Published: 18 November 2026

Copyright: © 2026 by the authors. Licensee MDPI, Basel, Switzerland. This article is an open access article distributed under the terms and conditions of the Creative Commons Attribution (CC BY) license.

1. Introduction

Ischemic brain injury develops when cerebral perfusion declines below the level required to maintain neuronal homeostasis. It remains one of the largest contributors to mortality and to acquired disability worldwide [1]. Within minutes of perfusion failure, energy depletion triggers excitotoxic and mitochondrial cascades that generate reactive oxygen species. The resulting oxidative and inflammatory injury drives neuronal death

and disrupts blood–brain barrier integrity [2,3]. The same sequence also occurs outside the acute occlusive setting owing to chronic cerebral hypoperfusion. This condition sustains the generation of reactive oxygen species and pro-inflammatory mediators, which aggravate neuronal damage [4].

Despite decades of intensive research, progress in developing drugs to protect the nervous system has been slow, and few have become part of routine clinical care. Edaravone, a free radical scavenger, is approved for acute ischemic stroke in Japan [5]. Moreover, China's National Medical Products Administration approved the fixed combination of edaravone with dexborneol in July 2020, and it is widely prescribed for this indication [6]. Randomized trials, including a phase III trial, of the latter have been reported in patients with acute ischemic stroke. Recent meta-analyses regard it as a neuroprotective strategy while noting the limitations of the available evidence [7,8]. Notably, edaravone-dexborneol combines a free radical scavenger with an anti-inflammatory agent. Thus, the clinical development of this combination supports the principle that targeting more than one arm of the ischemic cascade is more effective than targeting a single pathway. Outside these agents, the only acute therapy of proven benefit remains reperfusion, achieved either by intravenous thrombolysis or by mechanical thrombectomy. However, it can be offered only to the minority of patients who reach a stroke-ready hospital within a narrow time window [2,9]. Moreover, neuroprotective agents are effective only when treatment starts early [10]. Therefore, the short interval available for intervention creates a demand for rapid drug delivery to the brain.

A combination of agents targeting discrete cascades may be more effective than targeting a single pathway. Olmesartan medoxomil belongs to the angiotensin receptor blockers, a class of selective antagonists of the angiotensin II type-1 receptor. This blockade improves cerebrovascular autoregulation, reduces NADPH oxidase-generated oxidative stress, and suppresses inflammation and microglial activation [11–13]. Moreover, angiotensin receptor blockade reduced the infarct volume and improved functional recovery in experimental ischemic stroke [14,15]. Apigenin (4′,5,7-trihydroxyflavone) is a flavone present in the human diet, with chamomile, celery, and parsley among its principal sources [16]. Among the dietary flavonoids, it was selected because its neuroprotective activity has been demonstrated in the same models of cerebral ischemia/reperfusion injury used to evaluate angiotensin receptor blockers, and because its three phenolic hydroxyl groups, compared with five in quercetin, give it the greater lipophilicity required for incorporation into a lipid-based vehicle. In ischemic stroke models, apigenin reduced the infarct volume, improved neurological scores, and attenuated post-stroke cognitive deficits [17,18]. Consequently, combining the two drugs addresses vascular and inflammatory injury at the receptor level, along with oxidative and apoptotic damage within the neuron itself.

Unfortunately, the limited water solubility of olmesartan medoxomil (7.2 μg/mL at 298 K) and apigenin (1.35–2.16 μg/mL) hinders their delivery by the conventional oral route [19,20]. Alternatively, the non-invasive intranasal route can circumvent these constraints. Therapeutic molecules delivered to the olfactory mucosa can migrate along the olfactory nerve toward the olfactory bulb and deeper brain regions. Moreover, absorption across the respiratory mucosa provides access to the brainstem along the trigeminal pathway [21]. These pathways can deliver drug to the central nervous system within minutes, bypass the blood–brain barrier, and reduce systemic exposure and peripheral effects [22,23].

Self-nanoemulsifying drug delivery systems (SNEDDS) consist of an isotropic blend of oil, surfactant, and cosolvent. They yield a fine oil-in-water nanoemulsion upon aqueous dispersion [24,25]. Because the drug remains dissolved inside the nanosized lipid core, a large effective surface area becomes available and the risk of in situ precipitation is reduced [26,27].

The selection of a self-nanoemulsifying vehicle for nasal application follows from the properties of the two drugs. Both dissolve poorly in water. In a water-based nasal preparation, they would remain as particles that must dissolve before they can pass through the nasal tissue. A self-nanoemulsifying system presents both drugs in dissolved form within nanosized droplets, removing the dissolution step and maintaining a high concentration gradient at the mucosal surface. Moreover, the small volume that can be administered to the nasal cavity requires a vehicle with high solubilization capacity. Consequently, the intended dose fits within that volume.

SNEDDS components are usually selected using a screening solubility approach. However, the solubility of a drug depends on the relative proportions of the components. Therefore, these proportions are treated as mixture variables, and their effect on solubility is modeled by a mixture design [28]. Herein, Stat-Ease 360 software was used to model the influence of component proportions on drug solubility and identify the optimum composition [29].

Intranasal nanoemulsion systems have been described for angiotensin receptor blockers, the closest being a thermoresponsive in situ nanoemulgel of azilsartan medoxomil for nose-to-brain delivery in dementia, and for pairs of neuroprotective polyphenols such as curcumin and quercetin. In each case, the vehicle composition was established by screening candidate excipients individually or using a factorial design that treats the components as independent factors. The present work differs in two respects: an angiotensin receptor blocker is co-loaded with a flavone in a single intranasal self-nanoemulsifying vehicle, and the composition of that vehicle is defined by a constrained mixture model of the component proportions rather than by one-factor-at-a-time screening or a factorial design, neither of which accounts for the constant-sum constraint among the components [30,31].

The present work hypothesized that the solubility of olmesartan medoxomil and apigenin in a self-nanoemulsifying vehicle is governed by the relative proportions of surfactant, cosolvent, and oil rather than by the identity of any single component. A constrained mixture model of those proportions would identify a composition that simultaneously maximizes the solubilization capacity for both drugs and enhances their transport across nasal mucosa relative to a suspension. The work was carried out in four phases. First, the oil, the cosolvent, and the surfactant were selected based on solubility and transmittance measurements. Second, the influence of the three components on the solubility of both drugs was modeled using a constrained mixture design. Third, an optimum composition was selected to achieve the highest attainable solubilization capacity for both drugs and was verified experimentally against the predicted values. Finally, the transmucosal transport of the optimized formulation was compared with that of a conventional drug suspension using excised goat nasal mucosa.

2. Materials and Methods

2.1. Materials

Riyadh Pharma (Riyadh, Saudi Arabia) kindly donated olmesartan medoxomil, and apigenin was purchased from Beijing Mesochem Technology Co. Pvt. Ltd. (Beijing, China). Cremer Oleo GmbH & Co. KG (Hamburg, Germany) supplied two lipids, Imwitor® 308 (glyceryl monocaprylate) and Miglyol® 810 N (medium-chain triglycerides), while Gattefossé (Saint-Priest, France) supplied Peceol™ (glyceryl monooleate) and Labrasol® ALF (caprylocaproyl polyoxyl-8 glycerides). Soybean oil was obtained from John L. Seaton & Co. Ltd. (Croda International Plc., East Yorkshire, UK) and oleic acid from Avonchem (Cheshire, UK). Kolliphor® EL (polyoxyl 35 castor oil) and Kollisolv® PEG 400 (poly(ethylene glycol) 400) were products of BASF (Ludwigshafen, Germany). Tween™ 80 (polysorbate 80) was obtained from Loba Chemie (Mumbai, India), Tween™ 60 (polysorbate 60) and Tween™

85 (polysorbate 85) from Merck-Schuchardt OHG (Hohenbrunn, Germany), and propylene glycol from Winlab Laboratory (Leicestershire, UK). Acetonitrile was obtained from AppliChem Panreac (Darmstadt, Germany), and ammonium formate from Sigma-Aldrich (St. Louis, MO, USA). Distilled water was prepared in-house utilizing a PURELAB purification system (ELGA LabWater, Veolia Water Technologies, High Wycombe, UK).

2.2. Mixture Design of Experiments and Statistical Modeling

A constrained mixture design was applied because the three components of an SNEDDS are dependent. This means their proportions must add up to a fixed total, so any change in one necessarily alters the remaining two. The selected SNEDDS components, namely Kolliphor EL (A), poly(ethylene glycol) 400 (B), and Imwitor 308 (C), were accordingly considered as mixture components rather than independent factors. The impact of these three components on the solubility of apigenin and olmesartan medoxomil in the resulting formulations was considered as responses. The proportion of each component was selected in the following ranges: 40–70% *w*/*w* for the surfactant, 5–30% *w*/*w* for the cosolvent, and 20–40% *w*/*w* for the oil. These limits were set so that the surfactant-to-oil ratio remained at or above 1:1, the ratio at which Imwitor 308 emulsified spontaneously in the screening study described in Section 2.6, so that the oil proportion remained high enough for the system to behave as a lipid-based formulation rather than an essentially oil-free system, and so that the cosolvent proportion stayed low enough to limit drug precipitation on aqueous dilution. Stat-Ease 360 software version 25.0.8 (Stat-Ease Inc., Minneapolis, MN, USA) recommended seventeen formulations to investigate how formulation components affect drug solubility. Table 1 presents the composition of the seventeen suggested formulations.

Model selection was based on the sequential sum of squares and the lack-of-fit test. Analysis of variance (ANOVA) at $\alpha = 0.05$ was then applied to the retained model, and its adequacy was assessed using externally studentized residuals. The Box–Cox diagnostic was inspected for each response, and no power transformation was indicated ($\lambda = 1$). Observations beyond the software-defined diagnostic limits were flagged as outliers and removed before final fitting. The signal-to-noise ratio was expressed as adequate precision, with values exceeding 4 regarded as sufficient for navigation within the design space.

Table 1. Composition of the seventeen formulations suggested by the constrained mixture design (% *w*/*w*).

Run	A: Kolliphor EL (%)	B: Poly(ethylene glycol) 400 (%)	C: Imwitor 308 (%)
1	61.78	9.77	28.45
2	47.23	22.55	30.22
3	66.92	13.08	20.00
4	45.73	14.27	40.00
5	58.54	5.00	36.46
6	53.98	16.30	29.72
7	53.29	22.96	23.75
8	60.69	19.31	20.00
9	53.98	16.30	29.72
10	51.69	8.31	40.00
11	47.38	30.00	22.62
12	53.98	16.30	29.72
13	40.00	26.50	33.50
14	58.54	5.00	36.46
15	70.00	5.88	24.12
16	47.38	30.00	22.62
17	40.00	26.50	33.50

2.3. Numerical Optimization and Verification

Stat-Ease 360 software was used to identify the component proportions that maximize the solubility of olmesartan medoxomil and apigenin, based on the fitted models. Candidate solutions were ranked by the overall desirability function, and the one closest to 1 was taken as the optimum formulation. The saturation solubility of olmesartan medoxomil and apigenin was measured in this formulation. The experimental means were then compared with the predicted means and their 95% prediction intervals. Validation was accepted once the experimental mean of a response fell within its calculated interval.

2.4. Preparation of the Formulations

2.4.1. Formulations of the Mixture Design

Preparation of the seventeen formulations began with accurate weighing of the three components into glass beakers. The components were placed in an incubator at 50 °C for at least 2 h, then mixed on an MMS-15Max multi-position magnetic stirrer (Joan Lab Equipment (Zhejiang) Co., Ltd., Huzhou, China) at 1000 rpm. Stirring continued until a clear and single-phase homogeneous formulation was obtained.

2.4.2. Loaded Optimized SNEDDS and Suspension

The optimized formulation was loaded with olmesartan medoxomil and apigenin at a loading concentration of 2.5 mg/g. The SNEDDS components and drugs were stirred on an MMS-15Max multi-position magnetic stirrer (Joan Lab Equipment (Zhejiang) Co., Ltd., Huzhou, China) at 1000 rpm for 2 h until both drugs dissolved. Dispersion of this loaded system in distilled water at 5% *w*/*v* produced a nanoemulsion containing 125 µg/mL of each drug. At this dispersion ratio, the concentrations in contact with the tissue are 2.62% *w*/*v* Kolliphor® EL, 1.38% *w*/*v* poly(ethylene glycol) 400, and 1.00% *w*/*v* Imwitor® 308. For the suspension, sodium carboxymethylcellulose was dispersed in distilled water at 2% *w*/*v* concentration. Sodium carboxymethylcellulose was included because both drugs are poorly water-soluble and sediment rapidly without it. Without it, a homogeneous donor preparation could not be maintained across the sampling period. Olmesartan medoxomil and apigenin were then incorporated into this dispersion at 125 µg/mL of each drug under continuous stirring.

2.5. Solubility Study

The saturation solubility of each drug was determined separately in both the screened vehicles and the mixture-design formulations. The oil and cosolvent were chosen based on the measured saturation solubility of the two drugs. The screened lipids covered distinct chemical classes: a free fatty acid (oleic acid), two monoglycerides differing in chain length (Imwitor 308 and Peceol), a medium-chain triglyceride (Miglyol 810), and a long-chain triglyceride (soybean oil). Propylene glycol and poly(ethylene glycol) 400 were selected as the candidate cosolvents. Each vehicle was placed in a 5 mL glass vial with an excess of drug and kept at a controlled temperature (23 ± 2 °C) under stirring on an MMS-15Max multi-position magnetic stirrer (Joan Lab Equipment (Zhejiang) Co., Ltd., Huzhou, China) at 1000 rpm for one day. The undissolved drug was then sedimented by centrifugation at 13,000 rpm for 15 min using a Hettich MIKRO 20 microcentrifuge (Andreas Hettich GmbH & Co. KG, Tuttlingen, Germany). An accurately weighed portion of the clear supernatant was transferred into a tared 2 mL microcentrifuge tube and diluted with 1.8 mL of acetonitrile. The drug concentration was then measured by ultra-high-performance liquid chromatography (UHPLC) after suitable dilution. The analysis was performed on a Thermo Scientific UltiMate 3000 ultra-high-performance liquid chromatographic system equipped with a photodiode array detector and controlled by Chromeleon software version 7 (Thermo

Fisher Scientific, Waltham, MA, USA). Separation was achieved on an Acquity BEH C18 column (1.7 µm, 2.1 × 50 mm) maintained at 25 °C. The mobile phase consisted of 10 mM ammonium formate and acetonitrile (72.6:27.4, *v*/*v*) delivered isocratically at a flow rate of 0.218 mL/min. The injection volume was 2 µL. Apigenin was monitored at 339 nm and olmesartan medoxomil at 257 nm, with retention times of 3.57 and 4.43 min, respectively.

2.6. Emulsification Study

Four surfactants from different chemical classes, namely Tween 60, Tween 85, Labrasol ALF, and Kolliphor EL, were examined for their ability to emulsify the chosen oil (Imwitor 308). Briefly, equal amounts of the surfactant and Imwitor 308 were combined and heated in an incubator at 50 °C to form a uniform system. This was visually identified as a single transparent phase with no separation on standing. Distilled water was added to this mixture at a 1:100 ratio to form nanoemulsion droplets. The dispersion transmittance was recorded at 638 nm against distilled water as a blank using a UV–Vis spectrophotometer (Ultrospec 2100 Pro, Amersham Biosciences, NJ, USA). Photographs documented the physical appearance of each dispersion, and all measurements were repeated three times. The physical appearance of each dispersion was classified based on measured transmittance: clear at 90% or above, slightly opalescent from 50% to below 90%, turbid from 0% to below 50%.

2.7. Characterization of the Optimized Formulation

The droplet size, the polydispersity index, and the zeta potential of the loaded optimized formulation were determined using a Zetasizer Nano ZS (Malvern Panalytical, Malvern, UK). They were dispersed in simulated nasal fluid (pH 5.5) at dilution ratios of 1:20, 1:50, and 1:100. Simulated nasal fluid was selected as the dispersion medium because its pH and its electrolyte content reproduce the conditions encountered at the nasal mucosa.

2.8. Stability of the Optimized Formulation

2.8.1. Dilution Stability

The loaded optimized formulation was dispersed in simulated nasal fluid (pH 5.5) at dilution ratios of 1:20, 1:50, and 1:100 and maintained at 25 °C for 6 h. The dispersions were inspected visually for turbidity, drug precipitation, and phase separation at 0, 1, 2, 4, and 6 h.

2.8.2. Thermodynamic Stability

The loaded optimized formulation was examined under three stress conditions. The test agent was compared with an untreated sample examined at time zero. One sample was centrifuged at 5000 rpm for 30 min. A second sample was subjected to three heating cycles at 50 °C. A third sample was subjected to three freeze–thaw cycles at −80 °C. After each condition, the formulation was inspected for phase separation, creaming, cracking, and drug precipitation. Formulations that remained clear, homogeneous and single-phase were considered to have passed the test.

2.9. Ex Vivo Nasal Permeation

2.9.1. Simulated Nasal Fluid

Sodium chloride (8.77 g), potassium chloride (2.98 g), and calcium chloride (0.59 g) were dissolved in distilled water to prepare the simulated nasal fluid (SNF). Tween 80 (1 g) was then added; the volume was completed to 1 L, and the pH was adjusted to 5.5 with 1.0 N hydrochloric acid or 1.0 N sodium hydroxide as required, monitored using a HI 2211 pH/ORP meter (Hanna Instruments, Woonsocket, RI, USA).

2.9.2. Permeation Study

The ex vivo permeation of olmesartan medoxomil and apigenin across freshly excised goat nasal mucosa was investigated [32,33]. The mucosal tissues were obtained from a licensed local abattoir and transported to the laboratory in cold normal saline. The mucosa was excised from the respiratory region of the nasal cavity and separated from the underlying cartilage and bone, rinsed with normal saline, and equilibrated in freshly prepared simulated nasal fluid (SNF; pH 5.5). The respiratory region was selected because it represents the major absorptive surface of the nasal cavity and is the tissue most commonly used for the ex vivo evaluation of nasal permeability. The membranes used for the two preparations were obtained from the same tissue and the same anatomical site and were evaluated in parallel under identical conditions. A Franz diffusion cell was employed for the permeation study. The excised nasal mucosa was mounted between the donor and receptor compartments with the mucosal side facing the donor. In total, 1 mL of the dispersed optimized formulation or of the drug suspension, each containing olmesartan medoxomil and apigenin (125 µg/mL of each drug), was introduced into the donor compartment, then sealed with Parafilm to prevent evaporation. The receptor compartment was filled with 12.5 mL of SNF containing 0.1% *w*/*v* Tween 80 to maintain sink conditions and incubated at 37 ± 0.5 °C and 400 rpm. Samples were withdrawn at predetermined time intervals (0.25, 0.5, 1, 2, 3, 4, and 6 h) [34,35] and immediately replaced with an equal volume of fresh SNF (pH 5.5). Three diffusion cells were set up for each preparation.

2.9.3. Calculation of Permeation Parameters

The cumulative amount permeated per unit area at each sampling time (Q_n) was calculated with correction for the drug removed at earlier samplings as $Q_n = (C_n \times V_R + V_S \times \Sigma C_i)/A$, where C_n is the receptor concentration at the n-th sampling, ΣC_i is the sum of the receptor concentrations at all preceding samplings, V_R is the receptor volume (12.5 mL), V_S is the sample volume (1 mL), and A is the effective diffusion area (0.785 cm^2). The cumulative amount permeated (µg/cm^2) was plotted against time to obtain the permeation profile. The steady-state flux (J_{ss}, µg/cm^2/h) was calculated as the slope of the linear regression of the cumulative amount permeated against time between 0.25 and 6 h. The apparent permeability coefficient (K_p, cm/h) was determined using Equation (1):

$$K_p = \frac{J_{ss}}{C_0} \quad (1)$$

where J_{ss} is the steady-state flux, and C_0 is the initial drug concentration in the donor compartment (125 µg/mL). The enhancement ratio (ER) was calculated as the mean J_{ss} of the optimized formulation divided by the mean J_{ss} of the free drug suspension. Permeation data are presented as mean ± SD.

3. Results and Discussion

The development of the intranasal SNEDDS was carried out in four successive phases. The components were first selected based on solubility and emulsification measurements. Second, the influence of their proportions on the solubility of both drugs was modeled utilizing a constrained mixture design. Third, desirability-function analysis identified the optimized formulation, which was verified experimentally. Finally, the transmucosal transport of the optimized formulation was compared with that of a conventional drug suspension across excised nasal mucosa.

3.1. Selection of the Oil Phase

The oil phase with a high solubilization capacity for olmesartan medoxomil and apigenin was selected based on measured drug solubility. This allows the intended dose to be accommodated in a small formulation volume and keeps both drugs dissolved within the dispersed nanoemulsion. Table 2 shows the values obtained in five oils of different chemical classes. The highest capacity for both drugs was measured in Imwitor 308, followed by Peceol. However, the remaining oils, namely oleic acid, Miglyol 810, and soybean oil, showed considerably lower solubilization capacity for both drugs.

Table 2. Solubility of apigenin and olmesartan medoxomil measured at saturation in the screened oils (mean ± SD, $n = 3$).

Oil	Chemical Class	Apigenin Solubility (mg/g)	Olmesartan Medoxomil Solubility (mg/g)
Oleic acid	Free fatty acid	0.09 ± 0.007	0.08 ± 0.004
Imwitor 308	Medium-chain monoglyceride	1.78 ± 0.073	1.23 ± 0.078
Peceol	Long-chain monoglyceride	0.63 ± 0.070	0.41 ± 0.019
Miglyol 810	Medium-chain triglyceride	0.14 ± 0.002	0.07 ± 0.003
Soybean oil	Long-chain triglyceride	0.06 ± 0.006	0.06 ± 0.002

This behavior could be attributed to the partially esterified glycerol backbone of Imwitor 308 and Peceol. In both oils, the two free hydroxyl groups remain available to donate and accept hydrogen bonds. These hydroxyl groups could interact with the phenolic hydroxyl moieties of apigenin and with the imidazole nitrogen and the aliphatic hydroxyl of olmesartan medoxomil. In contrast, complete esterification of triglycerides in soybean oil and Miglyol 810 impairs hydrogen-bond formation with the polar groups of apigenin and olmesartan medoxomil. A comparable dependence of drug solubility on the degree of esterification of the glycerol backbone was reported previously for dapagliflozin and febuxostat, where monoglycerides likewise exceeded triglycerides in solubilization capacity [36,37].

Oleic acid carries a free carboxyl group but nevertheless dissolved the smallest amount of either drug. Carboxylic acid groups associate with each other through pairs of hydrogen bonds and exist in the neat liquid largely as cyclic dimers and higher aggregates. Both the donor and the acceptor of the carboxyl group are therefore already engaged with a neighboring fatty acid molecule. The affinity of oleic acid for itself therefore exceeds its affinity for either drug. Hydrogen bonding with apigenin or olmesartan medoxomil would require disrupting this self-associated network. However, this is energetically unfavorable and explains why a free carboxyl group alone is not sufficient to solubilize either molecule. The superior solubilization capacity of Imwitor 308 over Peceol could be ascribed to its higher hydroxyl group content per mass. Therefore, Imwitor 308 was chosen as the oil phase. It should be noted that no oil dissolved more than 1.78 mg/g of either drug, so that at the 20% *w*/*w* oil proportion of the optimized composition the oil phase can account for at most 0.36 mg/g of apigenin and 0.25 mg/g of olmesartan medoxomil, about 3% of the capacity finally measured; the limited contribution of the oil is consistent with the low and negative coefficients obtained for Imwitor 308 in both mixture models.

3.2. Selection of the Cosolvent

Two cosolvents were compared to maximize the apigenin and olmesartan medoxomil loading within the formulation. As Table 3 shows, poly(ethylene glycol) 400 dissolved approximately five times more olmesartan medoxomil and six times more apigenin compared to propylene glycol. Consequently, poly(ethylene glycol) 400 was selected as the SNEDDS cosolvent. This difference could be ascribed to the lower polarity of poly(ethylene

glycol) 400 and to the ether oxygens distributed along its chain. This accepts hydrogen bonds from the phenolic hydroxyl groups of apigenin and from the hydroxyl and imidazole groups of olmesartan medoxomil. In contrast, propylene glycol has two hydroxyl groups on a three-carbon backbone. Because of this high hydroxyl density, the liquid is strongly polar and extensively self-associated through hydrogen bonding.

Table 3. Solubility of the two drugs in the screened cosolvents (mean ± SD, $n = 3$).

Cosolvent	Olmesartan Medoxomil Solubility (mg/g)	Apigenin Solubility (mg/g)
Poly(ethylene glycol) 400	14.92 ± 1.02	19.88 ± 0.23
Propylene glycol	2.90 ± 0.55	3.26 ± 0.12

3.3. Selection of the Surfactant

Emulsification capacity was used as the criterion for selecting the surfactant [38]. Four surfactants were screened for this purpose, namely Tween 60, Tween 85, Labrasol ALF, and Kolliphor EL. The dispersions formed by Imwitor 308 with each surfactant are shown in Figure 1, and their transmittance values appear in Table 4. Turbid dispersions were produced with Labrasol ALF and Tween 85, consistent with their low transmittance. This indicates the formation of coarse droplets and poor emulsification efficiency. For Tween 85, this could be attributed to its three unsaturated oleate chains. This provides a bulky geometry that hinders close packing at the oil–water interface. Similarly, Labrasol ALF contains a fraction of di- and triglycerides that are poorly surface active, which limits droplet-size reduction. On the other hand, Tween™ 60 produced a slightly opalescent dispersion with intermediate transmittance. Finally, Kolliphor EL gave a visually clear dispersion of the highest transmittance. This indicates a pronounced ability to emulsify Imwitor 308 and to generate droplets in the nanometric range [24,39]. Therefore, Kolliphor EL was selected as the surfactant of the SNEDDS.

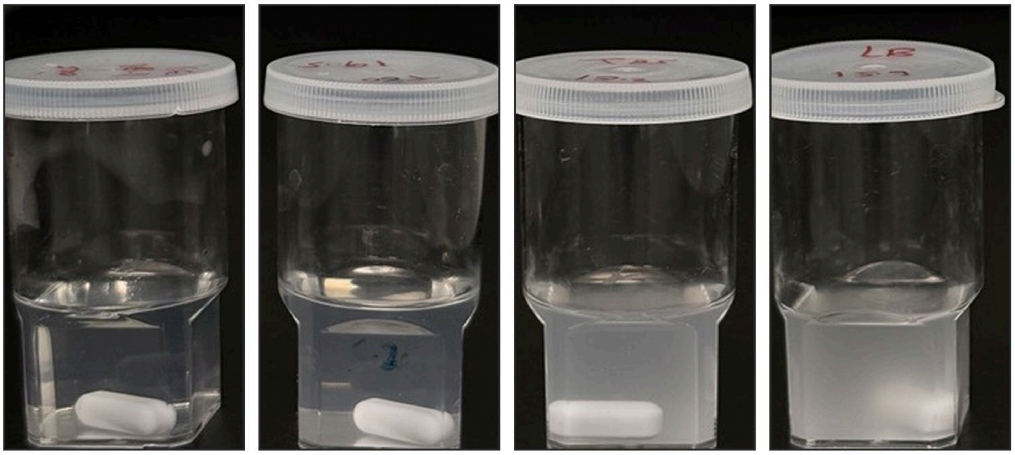


Figure 1. Physical appearance of the dispersions formed by Imwitor® 308 with (**a**) Kolliphor® EL, (**b**) Tween™ 60, (**c**) Tween™ 85, and (**d**) Labrasol® ALF after dilution 1:100 in distilled water.

Table 4. Transmittance and physical appearance of the dispersions formed by Imwitor 308 with each surfactant (mean ± SD, $n = 3$).

Surfactant	Transmittance (%)	HLB	Physical Appearance
Kolliphor EL	92.3 ± 0.23	12–14	Clear
Tween 60	82.1 ± 0.12	14.9	Slightly opalescent
Tween 85	18.3 ± 0.17	11.0	Turbid
Labrasol ALF	10.1 ± 0.10	12	Turbid

Table 4 presents the hydrophilic–lipophilic balance values of the four screened surfactants. All four fall within the 8 to 18 range assigned to oil-in-water emulsifiers. Thus, this parameter alone does not discriminate between them. Indeed, Tween™ 60 possesses the highest balance value of the four surfactants, yet produced a dispersion of lower transmittance than Kolliphor® EL. The emulsification behavior observed could therefore be ascribed to the molecular geometry of each surfactant and to the compatibility of its lipophilic moiety with the medium-chain monoglyceride constituting the oil phase, rather than to the balance value alone.

3.4. Experimental Responses and Model Diagnostics

Various statistical analyses were performed using Stat-Ease 360 software to select an appropriate model and to study the interactions between the components. Initial evaluation of the data showed that linear and quadratic models were suitable for apigenin and olmesartan medoxomil solubility, respectively. Table 5 presents the lack of fit obtained for each selected model. The results showed a non-significant lack of fit for apigenin solubility, with no recommendation for data transformation based on the Box–Cox analysis shown in Figure 2a. Moreover, all seventeen runs of the apigenin dataset remained within the diagnostic limits based on externally studentized residuals plotted against predicted values (Figure 3a). In contrast, the quadratic model for olmesartan medoxomil solubility showed a significant lack of fit (Table 5), and the Box–Cox analysis (Figure 2b) did not recommend data transformation. Further diagnostic analysis of the externally studentized residuals plotted against predicted values showed that three runs were flagged as outliers (Figure 3b). Therefore, the outlier points (runs 3, 8 and 15) were excluded, and the analysis was performed on the remaining fourteen runs. A quadratic model was suggested and showed a non-significant lack of fit, with no need for data transformation based on the Box–Cox analysis shown in Figure 2c. Moreover, externally studentized residuals plotted against predicted values in a diagnostic analysis showed that all fourteen runs were randomly distributed within the limits (Figure 3c). The exclusion was applied only to the olmesartan medoxomil model. The apigenin model was fitted to all seventeen runs because none exceeded the diagnostic limits (Figure 3a). Moreover, we evaluated a response transformation before removing any observations. The Box–Cox analysis of the olmesartan medoxomil response with all seventeen runs retained indicated that no power transformation was warranted (Figure 2b). Transforming the response therefore could not resolve the significant lack of fit, so we applied the diagnostic criterion defined in Section 2.2.

Table 5. Lack of fit of the model selected for each response.

Response and Model	*n*	Lack-of-Fit *p*-Value	Significance
Apigenin, linear	17	0.8024	Not significant
Olmesartan medoxomil, quadratic (before exclusion)	17	0.0015	Significant
Olmesartan medoxomil, quadratic (after exclusion)	14	0.1357	Not significant

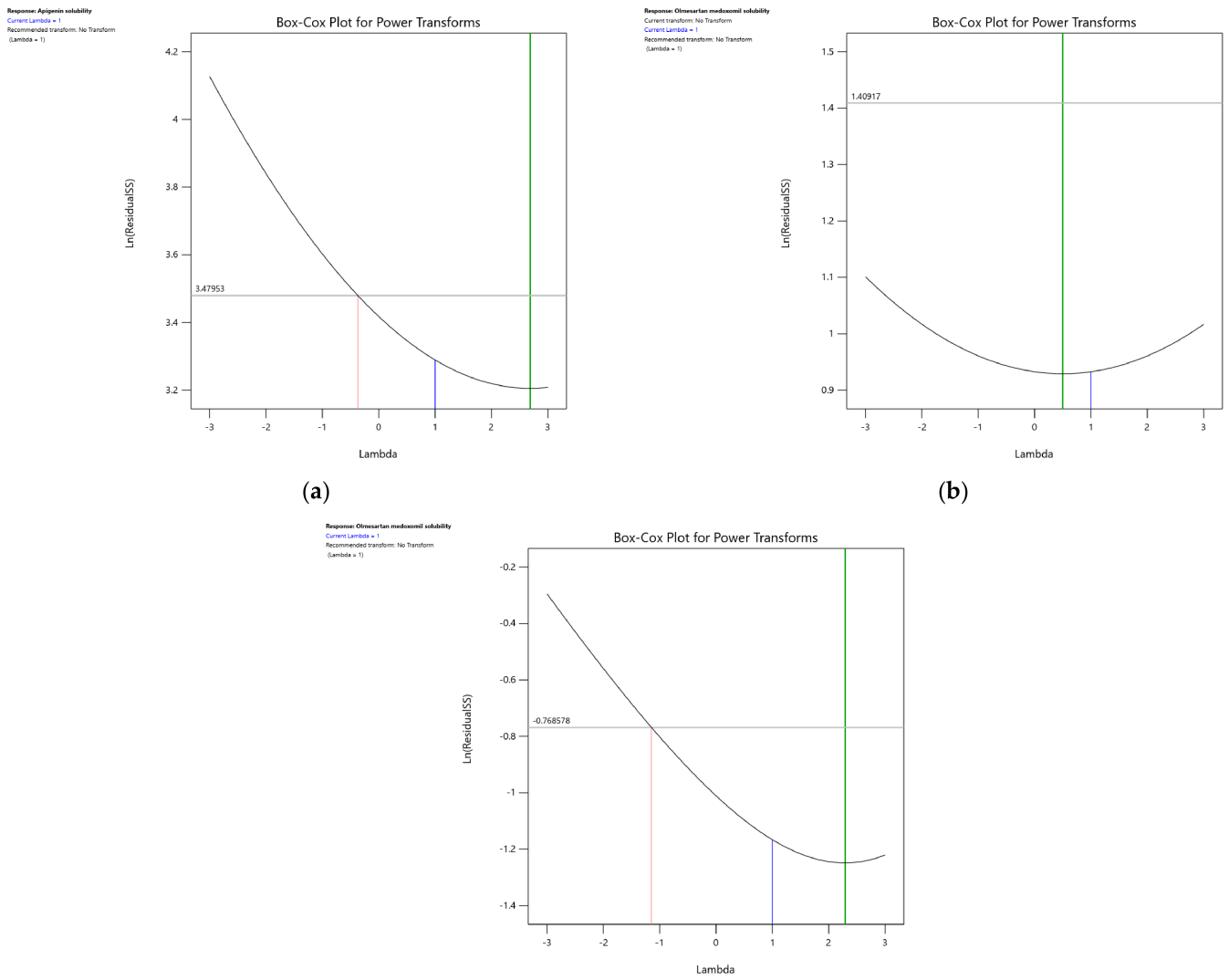


Figure 2. Box–Cox plots for (**a**) apigenin solubility including all seventeen runs, (**b**) olmesartan medoxomil solubility with the outliers retained, and (**c**) olmesartan medoxomil solubility after their exclusion.

3.5. Apigenin Solubility

Apigenin solubility ranged from 6.33 to 11.96 mg/g across the seventeen formulations. Table 6 summarizes the component effects quantified along Cox directions. The model showed an adequate precision of 5.33. Figure 4a shows a contour plot for the overall impact of the three components on apigenin solubility. Moreover, the trace plot in Figure 4b shows the impact of each component on apigenin solubility. Kolliphor EL exerted a positive effect on apigenin solubility, as indicated by the direction of its slope (Figure 4b) and the positive sign of its component effect (Table 6). The steep slope and the large magnitude of its component effect reveal a pronounced influence on apigenin solubility. This reflects its dominant role in solubilizing apigenin within the SNEDDS formulation. In contrast, Imwitor 308 showed the opposite behavior, as indicated by a descending slope (Figure 4b) and a negative component effect (Table 6). The steepness of this slope and the large negative effect value indicate a pronounced decline in apigenin solubility. In addition, statistical analysis revealed a non-significant ($p > 0.05$) impact of poly(ethylene glycol) 400 on apigenin solubility. However, the positive direction of its slope and the positive value of its component effect indicate a

modest augmenting influence on apigenin solubility. Apigenin solubility at any level of the three components could be predicted using Equation (2):

$$\text{Apigenin solubility} = 0.143638\ (\text{Kolliphor EL}) + 0.110377\ (\text{poly(ethylene glycol) 400}) - 0.009435\ (\text{Imwitor 308}) \quad (2)$$

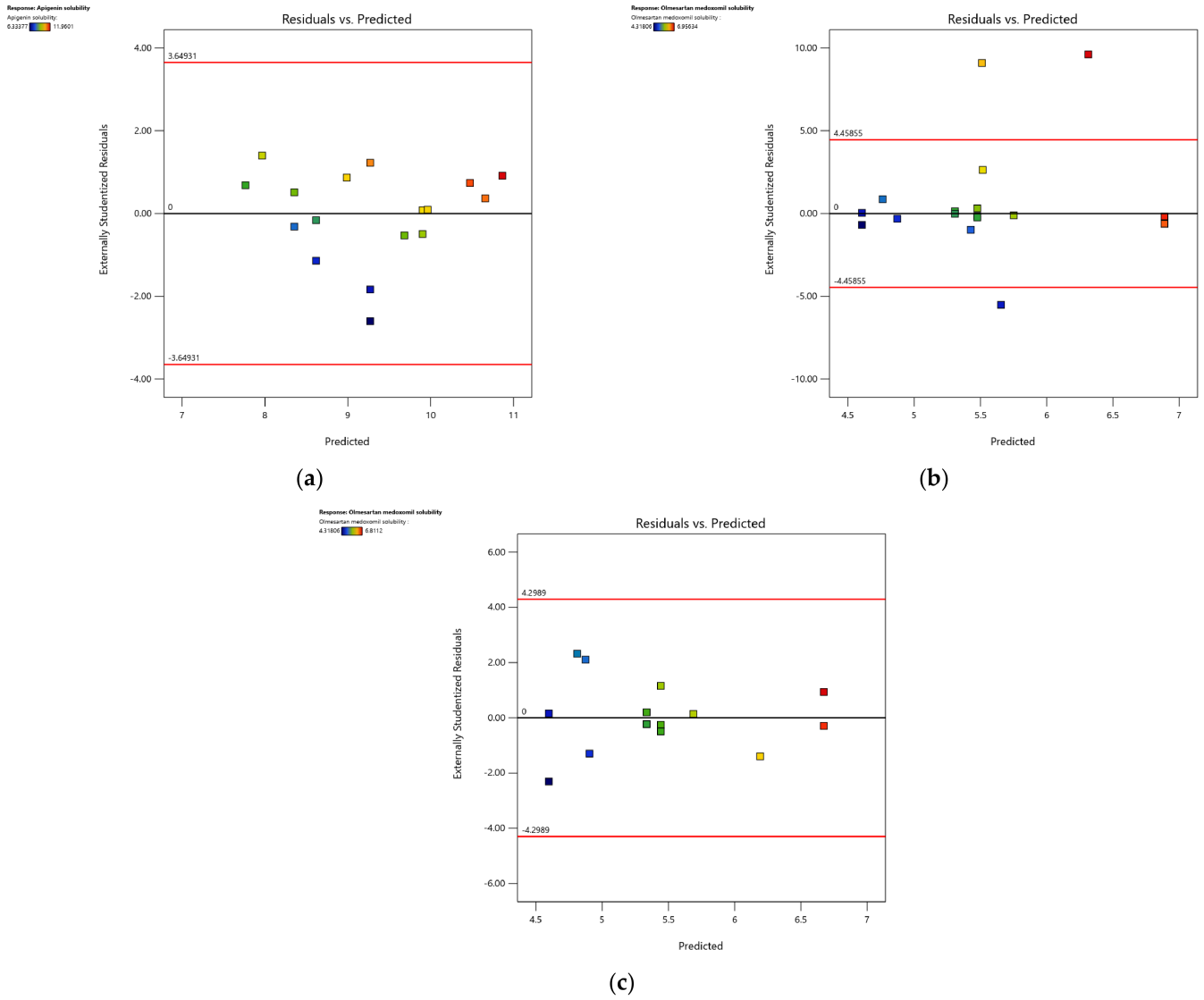
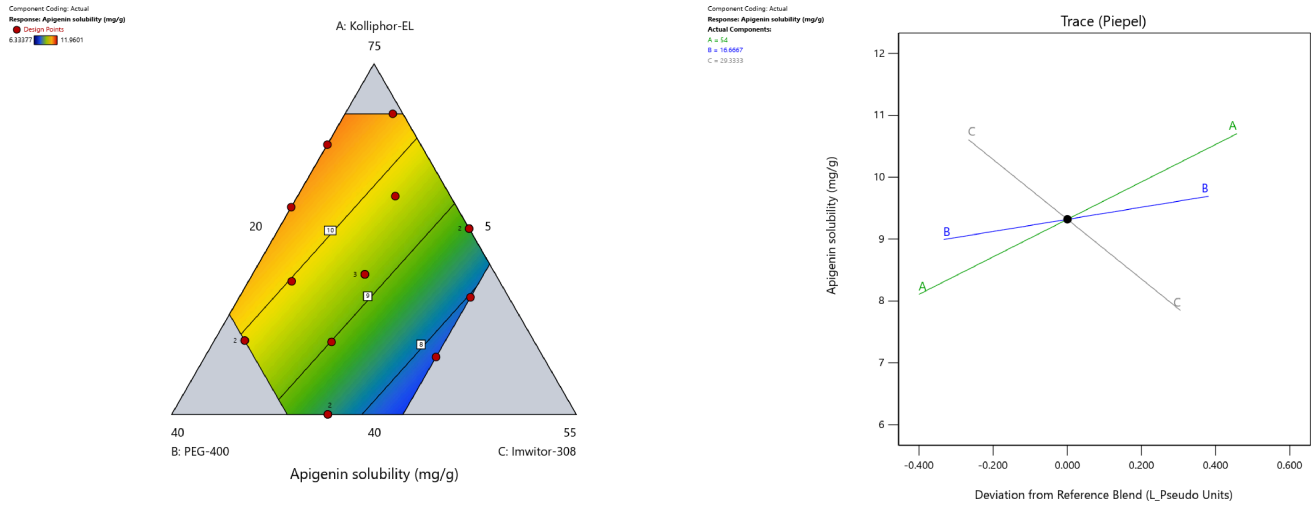


Figure 3. Externally studentized residuals plotted against predicted values for (**a**) apigenin solubility including all seventeen runs, (**b**) olmesartan medoxomil solubility with the outliers retained, and (**c**) olmesartan medoxomil solubility after their exclusion.

Table 6. Cox component effects for the linear model of apigenin solubility.

Component	Gradient in Reals	Component Effect (mg/g)	Gradient Std. Error	t for Gradient = 0	*p*-Value
A: Kolliphor EL	+10.97	+3.14	4.49	2.44	0.0285
B: Poly(ethylene glycol) 400	+2.06	+0.52	4.09	0.50	0.6218
C: Imwitor 308	−14.52	−2.90	5.39	−2.69	0.0175



(**a**) (**b**)

Figure 4. (**a**) Contour plot and (**b**) Piepel trace plot of apigenin solubility.

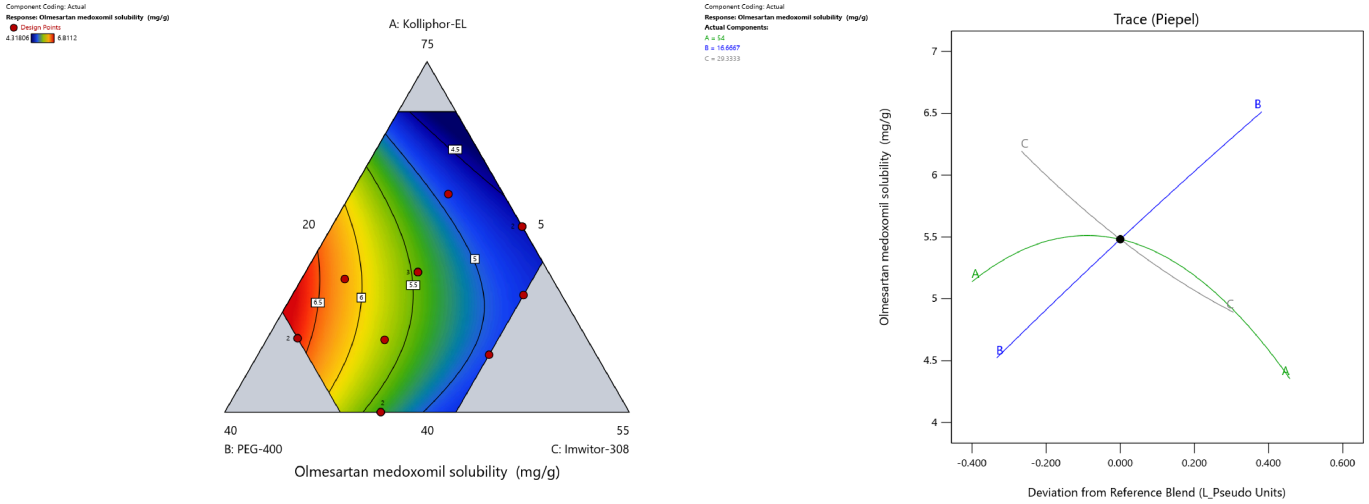
3.6. Olmesartan Medoxomil Solubility

Olmesartan medoxomil solubility ranged from 4.32 to 6.96 mg/g across the seventeen formulations. Table 7 summarizes the coefficient estimates obtained for the quadratic model in coded (pseudo-component) form, whereas Equation (3) is expressed in terms of the actual component proportions (% w/w). The model showed an adequate precision of 16.06. Figure 5a shows a contour plot for the overall impact of the three components on olmesartan medoxomil solubility, while the trace plot in Figure 5b shows the impact of each component. The ascending direction of its trace indicates a positive effect of poly(ethylene glycol) 400 on olmesartan medoxomil solubility. Moreover, the steep trace and the highest coefficient among the three components (7.24 mg/g) reveal a pronounced influence on olmesartan medoxomil solubility. In contrast, Imwitor 308 showed the opposite behavior, as indicated by the downward trend in its trace (Figure 5b) and a lower coefficient value (4.47 mg/g). This could result from the limited capacity of the oil phase to dissolve olmesartan medoxomil (1.23 mg/g), so that raising its proportion reduces the fraction available for the surfactant and the cosolvent. However, Kolliphor EL exhibited a curved trace with a maximum near the center of the design space, and its coefficient (3.67 mg/g) was the lowest of the three components. This indicates that its contribution is confined to a narrow range of proportions. The three binary terms were retained to preserve model hierarchy, but they are not statistically supported: the confidence intervals of the terms describing Kolliphor EL with poly(ethylene glycol) 400, Kolliphor EL with Imwitor 308, and poly(ethylene glycol) 400 with Imwitor 308 all span zero. No synergistic or antagonistic interaction is therefore claimed on the present data. Finally, olmesartan medoxomil solubility at any level of the three components could be predicted using Equation (3):

$$\begin{aligned}\text{Solubility (olmesartan medoxomil)} = {} & -0.006531\ (\text{Kolliphor EL}) + 0.085043\ (\text{poly(ethylene glycol) 400}) + \\ & 0.009209\ (\text{Imwitor 308}) + 0.002973\ (\text{Kolliphor EL} \times \text{poly(ethylene glycol) 400}) + 0.001814\ (\text{Kolliphor EL} \times \\ & \text{Imwitor 308}) - 0.002870\ (\text{poly(ethylene glycol) 400} \times \text{Imwitor 308})\end{aligned} \quad (3)$$

Table 7. Coefficient estimates of the olmesartan medoxomil quadratic model in coded factors.

Component	Coefficient Estimate (mg/g)	Standard Error	95% CI Low	95% CI High
A: Kolliphor EL	+3.67	1.13	+1.07	+6.27
B: Poly(ethylene glycol) 400	+7.24	0.40	+6.31	+8.17
C: Imwitor 308	+4.47	1.25	+1.58	+7.35
AB	+3.64	1.74	−0.38	+7.66
AC	+2.22	4.50	−8.15	+12.59
BC	−3.52	2.37	−8.97	+1.94



(**a**) (**b**)

Figure 5. (**a**) Contour plot and (**b**) Piepel trace plot of olmesartan medoxomil solubility.

3.7. Numerical Optimization

The optimization process was carried out to select the optimum formulation component proportions that achieve maximum solubility of apigenin and olmesartan medoxomil. Two solutions were suggested by the software, and the one with higher desirability was selected. It contained 52.33% *w*/*w* Kolliphor EL, 27.67% *w*/*w* poly(ethylene glycol) 400, and 20.00% *w*/*w* Imwitor 308, with an overall desirability of 0.848 (Figure 6).

3.8. Verification of the Optimized Formulation

The optimized formulation was prepared, and the measured solubility was compared with the predicted means together with their 95% prediction intervals (Table 8). The experimental mean of each response fell within its corresponding interval, which is consistent with the predictive accuracy of the developed models. This kind of verification is a core element of the quality-by-design framework because it provides direct empirical evidence that the model is reliable within the design space.

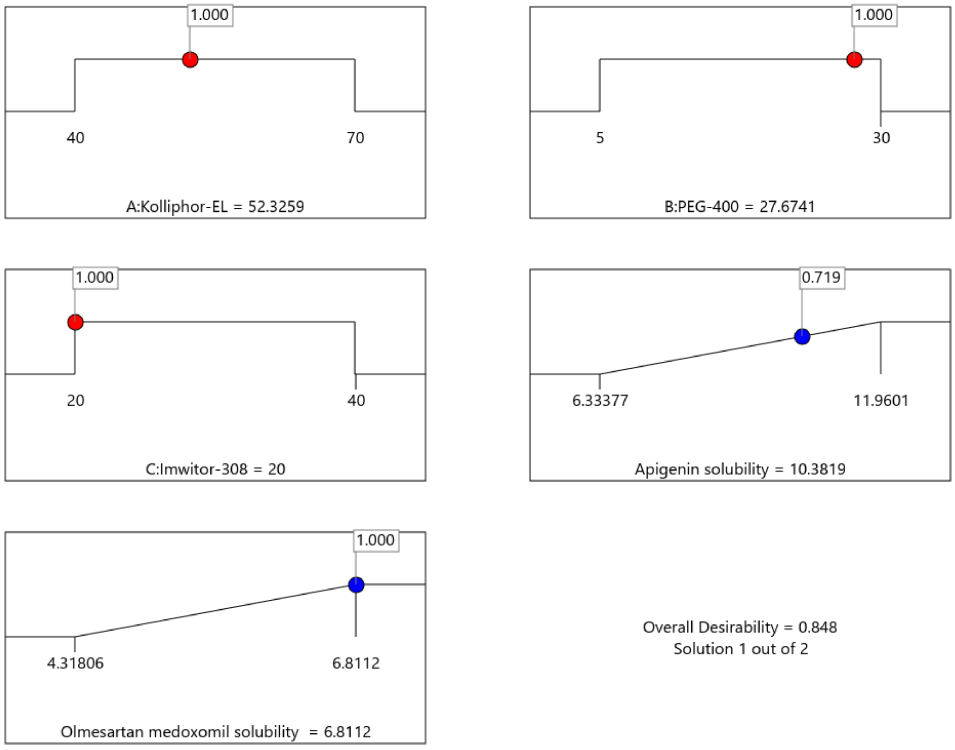


Figure 6. Desirability ramp plot of the optimized SNEDDS composition.

Table 8. Predicted and experimentally observed solubility of the optimized SNEDDS formulation.

Response	Predicted Mean	95% PI Low	95% PI High	Experimental Mean
Apigenin (mg/g)	10.38	8.16	12.60	11.82
Olmesartan medoxomil (mg/g)	6.81	6.23	7.39	6.91

3.9. Characterization of the Optimized Formulation

Table 9 presents the droplet size, the polydispersity index, and the zeta potential of the loaded optimized formulation across the examined dilution ratios in simulated nasal fluid. The droplet size ranged from 21.26 to 27.40 nm. Therefore, nanometric droplets were obtained at every dilution ratio. In addition, neither the pH nor the ionic strength of simulated nasal fluid prevented dispersion. The polydispersity index ranged from 0.357 to 0.398, indicating a polydisperse droplet population. The zeta potential ranged from −1.41 to +2.74 mV. These near-zero values could be ascribed to the non-ionic formulation components and to charge screening by the electrolytes of simulated nasal fluid.

Table 9. Droplet size, polydispersity index, and zeta potential of the loaded optimized formulation dispersed in simulated nasal fluid (pH 5.5).

Dilution Ratio	Droplet Size (nm)	Polydispersity Index	Zeta Potential (mV)
1:20	27.40 ± 1.05	0.357 ± 0.055	+2.74 ± 0.16
1:50	21.26 ± 3.91	0.398 ± 0.042	−0.68 ± 0.37
1:100	23.57 ± 2.41	0.395 ± 0.008	−1.41 ± 0.71

3.10. Stability of the Optimized Formulation

The diluted systems remained clear and transparent over the 6 h study period at all three dilution ratios. Furthermore, neither drug precipitation nor phase separation was

observed (Figure 7). Thus, the high cosolvent proportion of the optimized formulation did not promote drug precipitation upon aqueous dilution. Figure 8 also shows the physical appearance of the loaded optimized formulation at time zero and after each stress condition. The formulation was a clear, homogeneous, single-phase liquid at time zero (Figure 8a) and retained this appearance under every condition examined. Neither phase separation nor creaming was observed after centrifugation at 5000 rpm for 30 min (Figure 8b). This indicates the preconcentrate behaves as a thermodynamically stable isotropic mixture rather than as a kinetically stabilized dispersion. Neither cracking nor drug precipitation was observed after three heating cycles at 50 °C (Figure 8c) or three freeze–thaw cycles at −80 °C (Figure 8d). This indicates that the three components remained mutually miscible across the examined temperature range, and the repeated transitions did not induce irreversible demixing. Therefore, the developed system is physically stable under the examined conditions.

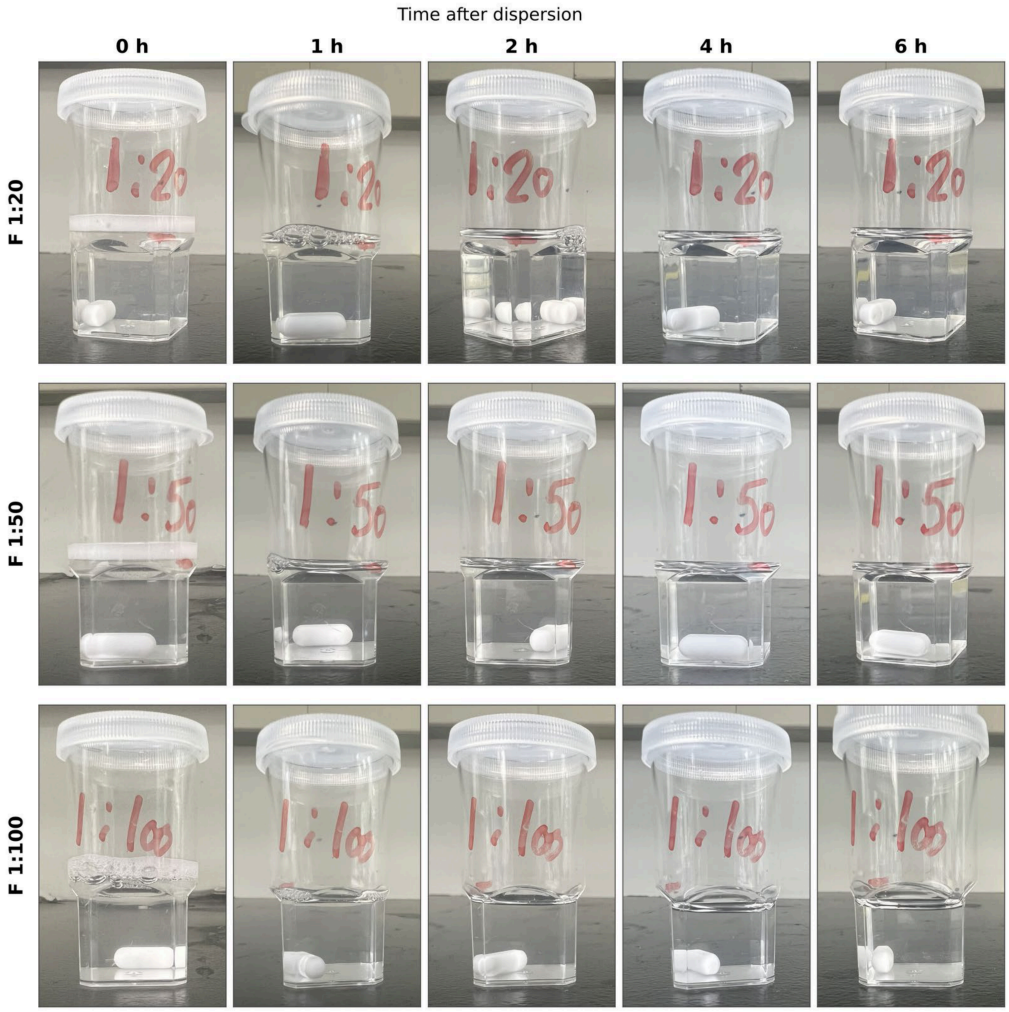


Figure 7. Visual appearance of the optimized formulation after dispersion in simulated nasal fluid (pH 5.5) at dilution ratios of 1:20, 1:50, and 1:100, photographed at 0, 1, 2, 4, and 6 h. All three dispersions remained clear and transparent, with no visible precipitation or phase separation over 6 h.

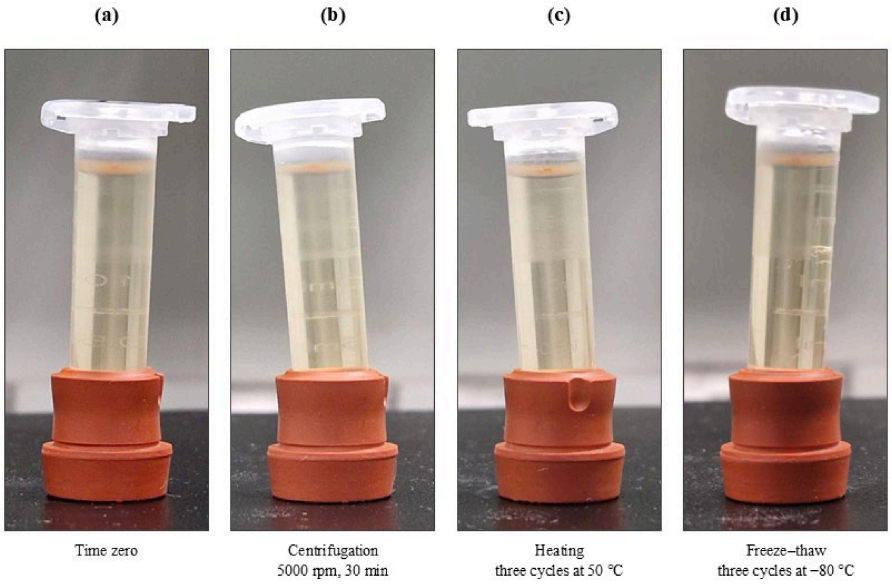


Figure 8. Physical appearance of the loaded optimized SNEDDS formulation (**a**) at time zero, (**b**) after centrifugation at 5000 rpm for 30 min, (**c**) after three heating cycles at 50 °C, and (**d**) after three freeze–thaw cycles at −80 °C.

3.11. Ex Vivo Permeation Study

The drug suspension was adopted as the reference preparation based on previously published methods. In this study, the transport of the formulated drug across excised nasal mucosa was compared with that of the unformulated drug suspended in an aqueous vehicle [40–42]. A mucosal nasal permeation study of the optimized formulations of olmesartan medoxomil and apigenin, as well as their free drugs, was performed. Figures 9 and 10 illustrate the cumulative amount of olmesartan medoxomil and apigenin permeated over time. The optimized formulation markedly increased the amount of these drugs that permeated across the excised nasal mucosa. The optimized olmesartan medoxomil formulation showed markedly higher permeation, reaching 54.46 ± 19.13 μg/cm^2 after 6 h, compared to the free drug suspension (5.07 ± 3.57 μg/cm^2). The optimized apigenin formulation also showed markedly higher permeation, reaching 68.18 ± 28.36 μg/cm^2 after 6 h, compared to the free drug suspension (1.10 ± 0.96 μg/cm^2). The higher permeation of both drugs from the optimized formulation could be attributed to the permeation-enhancing effect of the SNEDDS components [43].

The permeation study revealed that the optimized formulation markedly improved permeation parameters compared to the free-drug suspension. Table 10 displays the permeation parameters of olmesartan medoxomil and apigenin, including J_{ss} and K_p. The optimized formulation exhibited the highest J_{ss} values, reaching 8.46 ± 2.51 μg/cm^2/h for olmesartan medoxomil and 10.06 ± 3.63 μg/cm^2/h for apigenin. These values correspond to enhancement ratios of 9.92 and 54.61 relative to free olmesartan medoxomil (0.85 ± 0.68 μg/cm^2/h) and free apigenin (0.18 ± 0.17 μg/cm^2/h), respectively. Accordingly, the K_p values of the optimized formulation were higher than those of the free drug. The K_p of olmesartan medoxomil increased from (0.68 ± 0.54) × 10^{-2} cm/h for the free drug suspension to (6.77 ± 2.01) × 10^{-2} cm/h for the optimized formulation, while the K_p of apigenin increased from (0.15 ± 0.14) × 10^{-2} to (8.05 ± 2.90) × 10^{-2} cm/h. This behavior indicates the optimized formulation's superior ability to facilitate drug transport across the nasal mucosa. The enhancement may be attributed to the nanosized carrier system and improved drug solubilization.

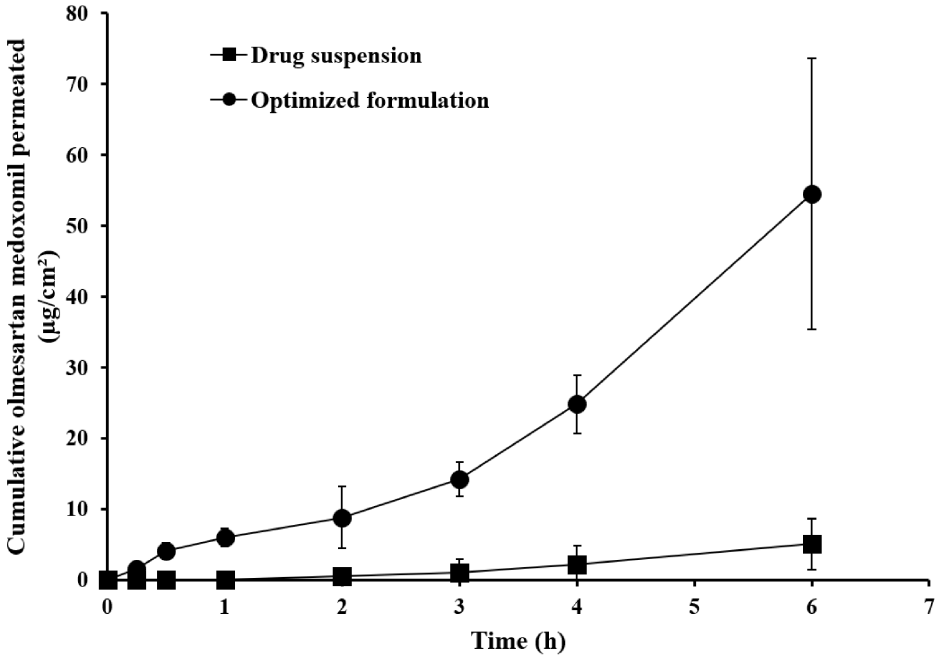


Figure 9. Ex vivo permeation profiles of olmesartan medoxomil across excised goat nasal mucosa from the dispersed optimized formulation and from the free drug suspension. Data are the mean ± SD.

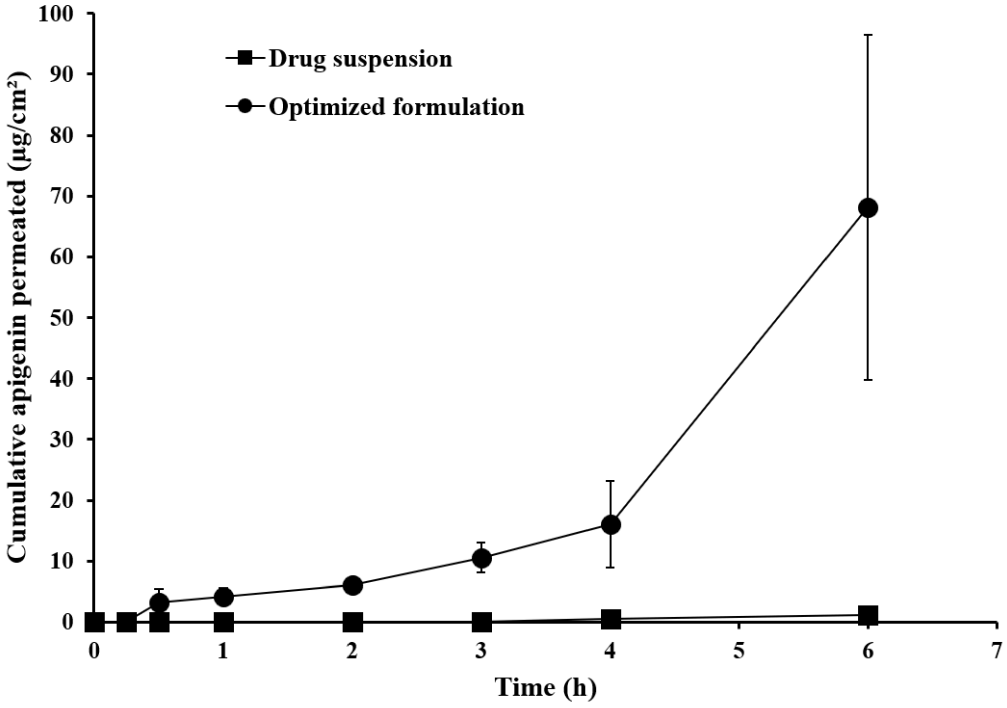


Figure 10. Ex vivo permeation profiles of apigenin across excised goat nasal mucosa from the dispersed optimized formulation and from the free drug suspension. Data are the mean ± SD.

Table 10. Ex vivo permeation parameters of olmesartan medoxomil and apigenin after intranasal application of the optimized SNEDDS formulation and the free drug suspension.

Parameters	Flux, J_{ss} ($\mu g/cm^2/h$)	Permeability Coefficient, $K_p \times 10^{-2}$ ($cm\ h^{-1}$)	Enhancement Ratio (ER)
	Olmesartan medoxomil		
Free drug	0.85 ± 0.68	0.68 ± 0.54	—
Optimized formulation	8.46 ± 2.51	6.77 ± 2.01	9.92
	Apigenin		
Free drug	0.18 ± 0.17	0.15 ± 0.14	—
Optimized formulation	10.06 ± 3.63	8.05 ± 2.90	54.61

J_{ss}, flux; K_p, permeability coefficient; ER, enhancement ratio. Data are the mean ± SD. J_{ss} was obtained from the linear regression of the cumulative amount permeated against time between 0.25 and 6 h. ER = mean J_{ss} of the optimized formulation/mean J_{ss} of the free drug.

Kolliphor® EL and poly(ethylene glycol) 400 have been combined in self-emulsifying systems developed for nasal administration. A previous study described poly(ethylene glycol) 400 as non-irritant to the nasal mucosa [44]. These systems are classified according to how much the ciliary beat frequency recovers after exposure and washout. A response is considered cilio-friendly if the frequency recovers to at least 75% of its initial value. It is considered cilio-inhibiting if the frequency recovers to more than 25% but less than 75%. It is considered ciliostatic if the frequency recovers to 25% or less [45]. Undiluted preconcentrates applied to ciliated epithelium ranged from cilio-friendly to ciliostatic depending on composition [44], and the effect of solubilizers such as poly(ethylene glycol) 400 on ciliary beat frequency in human nasal epithelial cells is concentration-dependent [46]. On respiratory epithelial cells, Kolliphor® EL at concentrations up to 10% v/v and poly(ethylene glycol) 400 up to 5% v/v did not compromise cell viability, membrane integrity or epithelial barrier function [47]. Moreover, a nanoemulsion containing Kolliphor EL, Tween 80, poly(ethylene glycol) 400, and medium-chain mono- and diglycerides developed for intranasal curcumin delivery showed no ciliotoxicity on sheep nasal mucosa [48]. In the present study, the system is dispersed at 5% w/v before administration. Therefore, the concentrations contacting the mucosa are 2.62% w/v Kolliphor® EL and 1.38% w/v poly(ethylene glycol) 400. These concentrations are below those tolerated by respiratory epithelial cells in vitro.

4. Conclusions

This work shows that the composition of a self-nanoemulsifying system intended to carry two drugs with dissimilar solubility behavior is best defined by treating its excipients as interdependent mixture components rather than by screening them one at a time. The mixture approach revealed that each drug depends on a different vehicle component, an insight single-excipient screening would not have exposed and that allowed one composition to accommodate both agents. Because the resulting models were verified experimentally, they provide a validated design space within which the formulation can be adjusted. For example, drug loading could be changed or an excipient grade substituted without repeating the full development program, in keeping with quality-by-design principles. From an applied standpoint, the optimized system converts two poorly water-soluble agents of complementary pharmacology into a single liquid preconcentrate intended for intranasal administration, and it markedly improves their transport across excised nasal mucosa compared with a conventional suspension. This establishes a practical formulation basis for the combined nasal delivery of an angiotensin receptor blocker and a flavonoid, and the same design strategy can be extended to other drug pairs whose co-formulation is limited by divergent solubility requirements.

Author Contributions: Conceptualization, A.Y.S.; data curation, E.M.E., A.Y.S. and M.M.B.; formal analysis, S.A., A.Y.S. and M.M.B.; methodology, A.Y.S. and M.M.B.; software, S.A. and A.Y.S.; validation, S.A., A.Y.S. and M.M.B.; investigation, E.M.E., S.A., A.Y.S. and M.M.B.; resources, E.M.E., A.Y.S., M.M.B. and M.A.A.; writing—original draft preparation, E.M.E., S.A., A.Y.S., M.M.B. and M.A.A.; writing—review and editing, E.M.E., A.Y.S., M.M.B. and M.A.A.; visualization, S.A., A.Y.S. and M.M.B.; supervision, E.M.E. and A.Y.S.; project administration, E.M.E. and A.Y.S.; funding acquisition, M.A.A. All authors have read and agreed to the published version of the manuscript.

Funding: The authors extend their appreciation to the Ongoing Research Funding program, Research Chairs (ORF-RC-2026-58-02), King Saud University, Riyadh, Saudi Arabia.

Institutional Review Board Statement: Nasal mucosa was obtained from goats slaughtered for human consumption at a licensed local abattoir; the tissue was a by-product of routine slaughter and no animal was killed for the purpose of this study.

Informed Consent Statement: Not applicable.

Data Availability Statement: The original contributions presented in this study are included in the article. Further inquiries can be directed to the corresponding author(s).

Acknowledgments: The authors extend their appreciation to the Ongoing Research Funding program, Research Chairs (ORF-RC-2026-58-02), King Saud University, Riyadh, Saudi Arabia. This research is an outcome of the memorandum of collaboration between College of Pharmacy, King Saud University and Riyadh Pharma Co. While preparing this manuscript, the authors utilized Claude (Opus, Anthropic, San Francisco, CA, USA) to edit the language and to help identify relevant literature. The authors verified every cited reference and every statement in the text against the primary sources. The authors reviewed and edited the generated output and take full responsibility for the manuscript content.

Conflicts of Interest: Riyadh Pharma Co. provided support in enhancing the laboratory infrastructure through the provision of laboratory equipment and provided the chemicals required to conduct this research. The company had no involvement in the study design, data collection, analysis or interpretation, manuscript preparation, or the decision to publish the results.

References

1. GBD 2021 Stroke Risk Factor Collaborators. Global, regional, and national burden of stroke and its risk factors, 1990–2021: A systematic analysis for the Global Burden of Disease Study 2021. *Lancet Neurol.* **2024**, *23*, 973–1003. [CrossRef] [PubMed]
2. Chamorro, Á.; Dirnagl, U.; Urra, X.; Planas, A.M. Neuroprotection in acute stroke: Targeting excitotoxicity, oxidative and nitrosative stress, and inflammation. *Lancet Neurol.* **2016**, *15*, 869–881. [CrossRef] [PubMed]
3. Qin, C.; Yang, S.; Chu, Y.-H.; Zhang, H.; Pang, X.-W.; Chen, L.; Zhou, L.-Q.; Chen, M.; Tian, D.-S.; Wang, W. Signaling pathways involved in ischemic stroke: Molecular mechanisms and therapeutic interventions. *Signal Transduct. Target. Ther.* **2022**, *7*, 215. Correction in *Signal Transduct. Target. Ther.* **2022**, *7*, 278. [CrossRef] [PubMed]
4. Rajeev, V.; Chai, Y.L.; Poh, L.; Selvaraji, S.; Fann, D.Y.; Jo, D.-G.; De Silva, T.M.; Drummond, G.R.; Sobey, C.G.; Arumugam, T.V.; et al. Chronic cerebral hypoperfusion: A critical feature in unravelling the etiology of vascular cognitive impairment. *Acta Neuropathol. Commun.* **2023**, *11*, 93. [CrossRef] [PubMed]
5. Watanabe, K.; Tanaka, M.; Yuki, S.; Hirai, M.; Yamamoto, Y. How is edaravone effective against acute ischemic stroke and amyotrophic lateral sclerosis? *J. Clin. Biochem. Nutr.* **2018**, *62*, 20–38. [CrossRef] [PubMed]
6. Li, J.; Cao, W.; Zhao, F.; Jin, P. Cost-effectiveness of edaravone dexborneol versus dl-3-n-butylphthalide for the treatment of acute ischemic stroke: A Chinese health care perspective. *BMC Public Health* **2024**, *24*, 436. [CrossRef] [PubMed]
7. Gao, H.; Tan, H.; Wang, J.; Yang, D.; Liu, Y.; Wu, T. Clinical efficacy of edaravone dexborneol in the treatment of acute ischemic stroke: Meta-analysis. *Front. Neurol.* **2025**, *16*, 1589307. [CrossRef] [PubMed]
8. Moghib, K.; Hefnawy, M.T.; Moawad, S.M.; Salomon, I.; Hamdi, A.; Uwishema, O.; Meshref, M. Efficacy and safety of edaravone dexborneol in acute ischemic stroke: Systematic review and meta-analysis. *Front. Neurol.* **2025**, *16*, 1649476. [CrossRef] [PubMed]
9. Pandian, J.D.; Gall, S.L.; Kate, M.P.; Silva, G.S.; Akinyemi, R.O.; Ovbiagele, B.I.; Lavados, P.M.; Gandhi, D.B.C.; Thrift, A.G. Prevention of stroke: A global perspective. *Lancet* **2018**, *392*, 1269–1278. [CrossRef] [PubMed]
10. Tymianski, M.; Hill, M.D.; Goyal, M.; Christenson, J.; Menon, B.K.; Swartz, R.H.; Adams, C.; Heard, K.; Kohli, Y. Safety and efficacy of nerinetide in patients with acute ischaemic stroke enrolled in the early window: A post-hoc meta-analysis of individual patient data from three randomised trials. *Lancet Neurol.* **2025**, *24*, 208–217. [CrossRef] [PubMed]

11. Rodriguez-Perez, A.I.; Dominguez-Meijide, A.; Lanciego, J.L.; Guerra, M.J.; Labandeira-Garcia, J.L. Dopaminergic degeneration is enhanced by chronic brain hypoperfusion and inhibited by angiotensin receptor blockage. *Age* **2013**, *35*, 1675–1690. [CrossRef] [PubMed]
12. Villapol, S.; Saavedra, J.M. Neuroprotective Effects of Angiotensin Receptor Blockers. *Am. J. Hypertens.* **2015**, *28*, 289–299. [CrossRef] [PubMed]
13. Nishimura, Y.; Ito, T.; Saavedra, J.M. Angiotensin II AT1 Blockade Normalizes Cerebrovascular Autoregulation and Reduces Cerebral Ischemia in Spontaneously Hypertensive Rats. *Stroke* **2000**, *31*, 2478–2486. [CrossRef] [PubMed]
14. Sato, K.; Yamashita, T.; Kurata, T.; Fukui, Y.; Hishikawa, N.; Deguchi, K.; Abe, K. Telmisartan Ameliorates Inflammatory Responses in SHR-SR after tMCAO. *J. Stroke Cerebrovasc. Dis.* **2014**, *23*, 2511–2519. [CrossRef] [PubMed]
15. Gutiérrez-Fernández, M.; Fuentes, B.; Rodríguez-Frutos, B.; Ramos-Cejudo, J.; Otero-Ortega, L.; Díez-Tejedor, E. Different protective and reparative effects of olmesartan in stroke according to time of administration and withdrawal. *J. Neurosci. Res.* **2015**, *93*, 806–814. [CrossRef] [PubMed]
16. Ghițu, A.; Schwiebs, A.; Radeke, H.H.; Avram, S.; Zupko, I.; Bor, A.; Pavel, I.Z.; Dehelean, C.A.; Oprean, C.; Bojin, F.; et al. A Comprehensive Assessment of Apigenin as an Antiproliferative, Proapoptotic, Antiangiogenic and Immunomodulatory Phytocompound. *Nutrients* **2019**, *11*, 858. [CrossRef] [PubMed]
17. Ling, C.; Lei, C.; Zou, M.; Cai, X.; Xiang, Y.; Xie, Y.; Li, X.; Huang, D.; Wang, Y. Neuroprotective effect of apigenin against cerebral ischemia/reperfusion injury. *J. Int. Med. Res.* **2020**, *48*, 0300060520945859. [CrossRef] [PubMed]
18. Tu, F.; Pang, Q.; Huang, T.; Zhao, Y.; Liu, M.; Chen, X. Apigenin Ameliorates Post-Stroke Cognitive Deficits in Rats Through Histone Acetylation-Mediated Neurochemical Alterations. *Med. Sci. Monit.* **2017**, *23*, 4004–4013. [CrossRef] [PubMed]
19. Shakeel, F.; Haq, N.; Alanazi, F.K.; Alsarra, I.A. Measurement and Correlation of Solubility of Olmesartan Medoxomil in Six Green Solvents at 295.15–330.15 K. *Ind. Eng. Chem. Res.* **2014**, *53*, 2846–2849. [CrossRef]
20. Zhang, J.; Liu, D.; Huang, Y.; Gao, Y.; Qian, S. Biopharmaceutics classification and intestinal absorption study of apigenin. *Int. J. Pharm.* **2012**, *436*, 311–317. [CrossRef] [PubMed]
21. Crowe, T.P.; Greenlee, M.H.W.; Kanthasamy, A.G.; Hsu, W.H. Mechanism of intranasal drug delivery directly to the brain. *Life Sci.* **2018**, *195*, 44–52. [CrossRef] [PubMed]
22. Kisku, A.; Nishad, A.; Agrawal, S.; Paliwal, R.; Datusalia, A.K.; Gupta, G.; Singh, S.K.; Dua, K.; Sulakhiya, K. Recent developments in intranasal drug delivery of nanomedicines for the treatment of neuropsychiatric disorders. *Front. Med.* **2024**, *11*, 1463976. [CrossRef] [PubMed]
23. Bourganis, V.; Kammona, O.; Alexopoulos, A.; Kiparissides, C. Recent advances in carrier mediated nose-to-brain delivery of pharmaceutics. *Eur. J. Pharm. Biopharm.* **2018**, *128*, 337–362. [CrossRef]
24. Date, A.A.; Nagarsenker, M.S. Design and evaluation of self-nanoemulsifying drug delivery systems (SNEDDS) for cefpodoxime proxetil. *Int. J. Pharm.* **2007**, *329*, 166–172. [CrossRef] [PubMed]
25. Buya, A.B.; Beloqui, A.; Memvanga, P.B.; Préat, V. Self-Nano-Emulsifying Drug-Delivery Systems: From the Development to the Current Applications and Challenges in Oral Drug Delivery. *Pharmaceutics* **2020**, *12*, 1194. [CrossRef] [PubMed]
26. Gursoy, R.N.; Benita, S. Self-emulsifying drug delivery systems (SEDDS) for improved oral delivery of lipophilic drugs. *Biomed. Pharmacother.* **2004**, *58*, 173–182. [CrossRef] [PubMed]
27. Pouton, C.W. Formulation of poorly water-soluble drugs for oral administration: Physicochemical and physiological issues and the lipid formulation classification system. *Eur. J. Pharm. Sci.* **2006**, *29*, 278–287. [CrossRef]
28. Scheffé, H. Experiments with Mixtures. *J. R. Stat. Soc. Ser. B (Methodol.)* **1958**, *20*, 344–360. [CrossRef]
29. Beg, S.; Swain, S.; Rahman, M.; Hasnain, M.S.; Imam, S.S. Application of Design of Experiments (DoE) in Pharmaceutical Product and Process Optimization. In *Pharmaceutical Quality by Design*; Beg, S., Hasnain, M.S., Eds.; Elsevier: Amsterdam, The Netherlands, 2019; pp. 43–64.
30. Karmakar, V.; Lim, W.M.; Gorain, B. Mechanistic insights into a thermoresponsive in situ nanoemulgel of azilsartan medoxomil for intranasal delivery: A promising nanotherapeutic approach to target dementia. *Biomater. Sci.* **2025**, *13*, 3853–3875. [CrossRef] [PubMed]
31. Vaz, G.; Clementino, A.; Mitsou, E.; Ferrari, E.; Buttini, F.; Sissa, C.; Xenakis, A.; Sonvico, F.; Dora, C.L. In Vitro Evaluation of Curcumin- and Quercetin-Loaded Nanoemulsions for Intranasal Administration: Effect of Surface Charge and Viscosity. *Pharmaceutics* **2022**, *14*, 194. [CrossRef] [PubMed]
32. Haasbroek-Pheiffer, A.; Van Niekerk, S.; Van der Kooy, F.; Cloete, T.; Steenekamp, J.; Hamman, J. In vitro and ex vivo experimental models for evaluation of intranasal systemic drug delivery as well as direct nose-to-brain drug delivery. *Biopharm. Drug Dispos.* **2023**, *44*, 94–112. [CrossRef] [PubMed]
33. Haasbroek-Pheiffer, A.; Viljoen, A.; Steenekamp, J.; Chen, W.; Hamman, J. An Ex vivo Investigation on Drug Permeability of Sheep Nasal Epithelial Tissue Membranes from the Respiratory and Olfactory Regions. *Curr. Drug Deliv.* **2024**, *21*, 115–125. [CrossRef]
34. Nasr, M. Development of an optimized hyaluronic acid-based lipidic nanoemulsion co-encapsulating two polyphenols for nose to brain delivery. *Drug Deliv.* **2016**, *23*, 1444–1452. [CrossRef] [PubMed]

35. Nagaraja, S.; Basavarajappa, G.M.; Karnati, R.K.; Bakir, E.M.; Pund, S. Ion-Triggered In Situ Gelling Nanoemulgel as a Platform for Nose-to-Brain Delivery of Small Lipophilic Molecules. *Pharmaceutics* **2021**, *13*, 1216. [CrossRef] [PubMed]
36. Sherif, A.Y.; Elzayat, E.M. Development of Bioresponsive Poloxamer-Based Self-Nanoemulsifying System for Enhanced Febuxostat Bioavailability: Solidification Strategy Using I-Optimal Approach. *Pharmaceutics* **2025**, *17*, 975. [CrossRef] [PubMed]
37. Sherif, A.Y.; Altamimi, M.A.; Elzayat, E.M. Implementation of a Potential Industrial Green, Economical, and Safe Strategy to Enhance Commercial Viability of Liquid Self-Nanoemulsifying Drug Delivery System. *Pharmaceutics* **2025**, *17*, 1461. [CrossRef]
38. Sherif, A.Y.; Elzayat, E.M.; Altamimi, M.A. Optimization of Glibenclamide Loaded Thermoresponsive SNEDDS Using Design of Experiment Approach: Paving the Way to Enhance Pharmaceutical Applicability. *Molecules* **2024**, *29*, 5163. [CrossRef] [PubMed]
39. Shahba, A.A.-W.; Mohsin, K.; Alanazi, F.K. Novel Self-Nanoemulsifying Drug Delivery Systems (SNEDDS) for Oral Delivery of Cinnarizine: Design, Optimization, and In-Vitro Assessment. *AAPS PharmSciTech* **2012**, *13*, 967–977. [CrossRef] [PubMed]
40. Shilakari, G.; Uppala, S.K.; Ganti, M.; Bhukya, S.; Asthana, A. Intranasal nanoemulsion-based in-situ gel containing dexlansoprazole: Formulation development, in-vitro and ex-vivo evaluation. *Drug Dev. Ind. Pharm.* **2026**, *52*, 1251–1272. [CrossRef] [PubMed]
41. Gad, S.R.; George, M.Y.; El-Gogary, R.I.; Hathout, R.M. Breaking Barriers: Intranasal Microemulsions for the Efficient Nose-to-brain Delivery of Glycyrrhetinic Acid. *AAPS PharmSciTech* **2026**, *27*, 112. [CrossRef] [PubMed]
42. Mahajan, H.S.; Mahajan, M.S.; Nerkar, P.P.; Agrawal, A. Nanoemulsion-based intranasal drug delivery system of saquinavir mesylate for brain targeting. *Drug Deliv.* **2014**, *21*, 148–154. [CrossRef] [PubMed]
43. Negi, M.; Amulya, E.; Phatale, V.; Kumar, R.; Srivastava, S. Nose-to-brain delivery of berberine-loaded nanoemulsion: Amelioration of brain targeting, behavioral, pharmacokinetic, and biodistribution insights for Alzheimer's intervention. *Biomater. Adv.* **2026**, *184*, 214835. [CrossRef] [PubMed]
44. Leichner, C.; Baus, R.A.; Jelkmann, M.; Plautz, M.; Barthelmes, J.; Dünnhaupt, S.; Bernkop-Schnürch, A. In vitro evaluation of a self-emulsifying drug delivery system (SEDDS) for nasal administration of dimenhydrinate. *Drug Deliv. Transl. Res.* **2019**, *9*, 945–955. [CrossRef] [PubMed]
45. Merkus, P.; Romeijn, S.G.; Verhoef, J.C.; Merkus, F.W.H.M.; Schouwenburg, P.F. Classification of Cilio-Inhibiting Effects of Nasal Drugs. *Laryngoscope* **2001**, *111*, 595–602. [CrossRef] [PubMed]
46. Vetter, A.; Augustijns, P.; Bernkop-Schnürch, A. Solubilizing agents in nasal formulations and their effect on ciliary beat frequency. *Toxicol. Vitr.* **2012**, *26*, 150–156. [CrossRef] [PubMed]
47. MacDonald, C.; Lyzenga, W.; Shao, D.; Agu, R.U. Water-soluble organic solubilizers for in vitro drug delivery studies with respiratory epithelial cells: Selection based on various toxicity indicators. *Drug Deliv.* **2010**, *17*, 434–442. [CrossRef] [PubMed]
48. Sood, S.; Jain, K.; Gowthamarajan, K. Optimization of curcumin nanoemulsion for intranasal delivery using design of experiment and its toxicity assessment. *Colloids Surf. B Biointerfaces* **2014**, *113*, 330–337. [CrossRef] [PubMed]

Disclaimer/Publisher's Note: The statements, opinions and data contained in all publications are solely those of the individual author(s) and contributor(s) and not of MDPI and/or the editor(s). MDPI and/or the editor(s) disclaim responsibility for any injury to people or property resulting from any ideas, methods, instructions or products referred to in the content.